

## Study of the Nonstoichiometry and Physical Properties of the $\text{Sr}_x\text{Dy}_{1-x}\text{FeO}_{3-y}$ Ferrite System

CHUL HYUN YO AND EUN SEOK LEE

*Department of Chemistry, Yonsei University, Seoul 120, Korea*

AND MOO SIL PYON

*Department of Chemical Engineering, Myong-Ji University, Seoul 121, Korea*

Received March 6, 1987; in revised form September 2, 1987

A series of samples in the  $\text{Sr}_x\text{Dy}_{1-x}\text{FeO}_{3-y}$  system ( $x = 0.00, 0.25, 0.50, 0.75,$  and  $1.00$ ) have been produced by heating the reactants to  $1200^\circ\text{C}$  in air under atmospheric pressure. Mohr salt analysis shows that  $\text{DyFeO}_3$  is a stoichiometric compound and that  $\text{Fe}^{4+}$  ions and oxygen deficiency compensate for the cation charge deficiency which is caused by substitution of  $\text{Sr}^{2+}$  at  $\text{Dy}^{3+}$  sites. X-ray powder diffraction assigns the compositions  $x = 0.00$  and  $0.25$  to the orthorhombic system and the compositions  $x = 0.50, 0.75,$  and  $1.00$  to the cubic system. The electrical conductivity sharply increases and the activation energy decreases with the presence of mixed iron valency. The Mössbauer spectra of the samples with  $x = 0.25$  and  $0.50$  are composed of two sets of six lines and a single broad peak for  $x = 0.75$ . © 1988 Academic Press, Inc.

### Introduction

Perovskite-type compounds have been extensively studied (1-5) because of their unique and interesting properties. These compounds are useful in many fields as laser host materials, thermistors, semiconductors, superconductors, etc. The orthoferrites with the formula  $R\text{FeO}_3$ , where  $R$  is a rare earth element, have the space group  $Pbnm (D_{2h}^{16})$  (1, 2). The crystal structure is a distorted perovskite with four equivalent iron ions per cell. The Mössbauer spectra of various orthoferrites have been studied between room temperature and Néel temperature ( $T_N$ ) by Eibschutz *et al.* (1), giving six-line spectra below  $T_N$  and an unsplit single line above  $T_N$ .

Among the ferrites with perovskite structures, the  $(\text{La}, \text{Sr})\text{FeO}_4$  system has been widely investigated. The conductivity after annealing in oxygen is higher than after annealing *in vacuo* due to the mixed-valence state of iron with both  $\text{Fe}^{3+}$  and  $\text{Fe}^{4+}$  (3). In the system  $\text{La}_{1-x}\text{Sr}_x\text{FeO}_3$  (4, 5) the valence state of the Fe atoms changes from the trivalent to the tetravalent state due to the substitution of Sr atoms at La sites. The change in the valence state and oxygen content may cause magnetic disordering. Accordingly, the Néel temperature of  $\text{LaFeO}_3$  (750 K) decreases as the  $x$  value is increased. This effect has been demonstrated by the study of the Mössbauer spectra (5). X-ray data and Mössbauer spectra for the system  $\text{Sr}_{1-x}\text{La}_x\text{FeO}_{2.5+x/2}$  ( $0.00 \leq x \leq 1.00$ )

prepared by firing at 1000°C in vacuum have been reported by Yamamura and Kiri-yama (6). In that study, the Brownmil-lerite-type structure at  $x = 0.30$  and the existence of a five-coordinated iron site surrounded by trigonal dipyramid of oxy-gen was suggested.

In the present study, solid solutions of the  $\text{Sr}_x\text{Dy}_{1-x}\text{FeO}_{3-y}$  system ( $x = 0.00, 0.25, 0.50, 0.75, \text{ and } 1.00$ ) were prepared and the cell parameters were ensured by powder X-ray diffraction. The mixed valence state was characterized by Mohr salt analysis and Mössbauer spectroscopy. Nonstoi-chiometric compositions were calculated from the chemical formula  $\text{Sr}_x\text{Dy}_{1-x}\text{Fe}_{1-\tau}^{3+}\text{Fe}_\tau^{4+}\text{O}_{3-y}$  (where  $y = (x - \tau)/2$ ). The electrical conductivity was found to increase with the formation of the mixed-valence state. This and the mechanism are discussed.

## Experimental Procedures

### (1) Sample Preparation

All the samples were prepared as fol-lows: The starting materials were  $\text{Dy}_2\text{O}_3$ ,  $\text{SrCO}_3$ , and  $\text{Fe}(\text{NO}_3)_3 \cdot 9\text{H}_2\text{O}$ , each of high purity. They were weighed in the desired proportions and dissolved in nitric acid. The solution was evaporated over a burner flame and then fired at 800°C for 4 hr in a platinum crucible. After being ground, mixed, heated at 1200°C in air for 10 hr and air quenched, the samples were weighed and studied by X-ray diffraction. This pro-cess was repeated three times in order to obtain homogeneous solid solutions.

Each powder sample was pressed into a pellet under a pressure of 2 ton/cm<sup>2</sup> for 2 min and all the pellets were sintered under the same conditions for study of the rela-tionship between the nonstoichiometric for-mula and electric conductivity.

### (2) X-ray Powder Patterns

X-ray diffraction studies of the samples were carried out using monochromatized

$\text{CuK}\alpha$  radiation. Comparing the  $d_{\text{cal}}$  value from least-squares calculation with the  $d_{\text{obs}}$  value from X-ray measurements, we con-firmed the indices of each line and then de-termined the crystal system, lattice param-eters, and volume of the unit cell (Table I).

### (3) Chemical Analysis

Titration of residual  $\text{Fe}^{2+}$  and 0.1 *N*  $\text{K}_2\text{Cr}_2\text{O}_7$  using Mohr salt gave the amount of  $\text{Fe}^{4+}$  and, from this value, the oxygen content of each sample.

### (4) Electrical Conductivity

Electrical conductivities of the samples have been measured by the four probe method in the temperature range 173 ~ 473 K. Independent measurements of volt-age and current were performed with the inner two probes connected to the potenti-ometer and the outer two probes to the electrometer. We used liquid nitrogen for the low temperature measurements. For the purpose of maintaining thermal equilib-rium, the temperature was raised at the rate of 1°C/min. The electrical conductivities were calculated using Laplume's equation (7).

### (5) Mössbauer Measurements

The Mössbauer spectra were accumu-lated using a spectrometer equipped with a

TABLE I  
LATTICE PARAMETERS, VOLUME, AND CRYSTAL  
SYSTEM FOR  $\text{Sr}_x\text{Dy}_{1-x}\text{FeO}_{3-y}$

Composition ( <i>x</i> )	Lattice parameters (Å)	Volume (Å <sup>3</sup> )	Symmetry
0.00	<i>a</i> 5.3040	56.47	Orthorhombic
	<i>b</i> 5.5871		
	<i>c</i> 7.6219		
0.25	<i>a</i> 5.3165	56.69	Orthorhombic
	<i>b</i> 5.5920		
	<i>c</i> 7.6255		
0.50	<i>a</i> 3.8636	56.67	Cubic
0.75	<i>a</i> 3.8718	58.04	Cubic
1.00	<i>a</i> 3.8659	57.78	Cubic

308-channel pulse-height analyzer. The source was cobalt-57 (dispersed in Rh) with 14.4 KeV  $\gamma$ -radiation. Absorbers with a diameter of 25.4 mm and a thickness of 0.5 mm were prepared from the highly ground oxide samples. We used  $\alpha$ -Fe as the velocity reference.

## Discussion

We confirmed that Dy<sup>3+</sup> could be replaced by Sr<sup>2+</sup> over the whole range of  $x = 0.00$  to 1.00 and that each sample was homogeneous. The X-ray powder patterns of the samples with  $x = 0.00$  and 0.25 were indexed on the basis of a distorted perovskite-type structure with orthorhombic symmetry, and for  $x = 0.50, 0.75,$  and 1.00 the symmetry changed to cubic. For the system SrFeO<sub>*x*</sub>, Watanabe (3) obtained mixtures of SrFeO<sub>2.5</sub> and SrFeO<sub>3.0</sub> in the range of  $x = 2.56$ – $2.73$ , but the sample SrFeO<sub>2.73</sub> prepared in this study was found to be homogeneous and cubic. The unit cell volume is plotted versus the composition in Fig. 1. Three main factors affect the cell volume: (a) substitution of Sr<sup>2+</sup> at Dy<sup>3+</sup> sites, (b) oxygen vacancies, and (c) formation of the mixed-valence state of Fe<sup>3+</sup> and Fe<sup>4+</sup>. Over the compositional range  $x = 0.00$ – $0.75$ , the unit cell volume increases

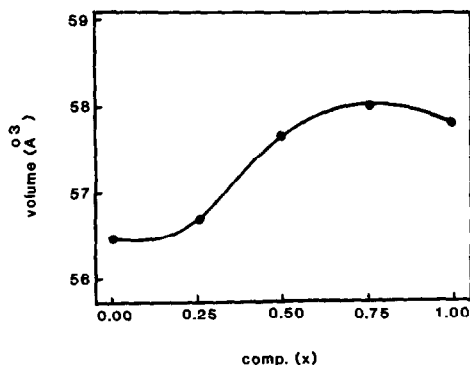


FIG. 1. Volume change with the increase in  $x$  value in the system Sr<sub>*x*</sub>Dy<sub>1-*x*</sub>FeO<sub>3-*y*</sub>.

TABLE II  
NONSTOICHIOMETRIC CHEMICAL FORMULAS OF THE  
Sr<sub>*x*</sub>Dy<sub>1-*x*</sub>Fe<sub>3+*τ*</sub>Fe<sub>4+</sub>O<sub>3-*y*</sub> SYSTEM ( $y = (x - \tau)/2$ )

Composition (x)	$\tau$ value	$y$ value	Chemical formula
0.00	0.00	0.00	DyFeO <sub>3</sub>
0.25	0.10	0.075	Sr <sub>0.25</sub> Dy <sub>0.75</sub> Fe <sub>0.90</sub> <sup>3+</sup> Fe <sub>0.10</sub> <sup>4+</sup> O <sub>2.925</sub>
0.50	0.16	0.17	Sr <sub>0.50</sub> Dy <sub>0.50</sub> Fe <sub>0.84</sub> <sup>3+</sup> Fe <sub>0.16</sub> <sup>4+</sup> O <sub>2.830</sub>
0.75	0.30	0.225	Sr <sub>0.75</sub> Dy <sub>0.25</sub> Fe <sub>0.70</sub> <sup>3+</sup> Fe <sub>0.30</sub> <sup>4+</sup> O <sub>2.775</sub>
1.00	0.46	0.27	SrFe <sub>0.54</sub> <sup>3+</sup> Fe <sub>0.46</sub> <sup>4+</sup> O <sub>2.730</sub>

with  $x$ . Thus, we concluded the factor  $a$  is predominant in this  $x$  range because the ionic radius of Sr<sup>2+</sup> (132 pm) is larger than that of Dy<sup>3+</sup> (105.2 pm). On the other hand, when  $x = 1.00$  a reduction in unit cell volume occurs probably due to factors  $b$  and  $c$ . It is known that the charge deficiency caused by the substitution of Sr<sup>2+</sup> for Dy<sup>3+</sup> can be compensated for by a change in the oxidation state of Fe, and by the formation of oxygen vacancies. As the samples were prepared in air at atmospheric pressure, a mixture of Fe<sup>3+</sup> and Fe<sup>4+</sup> valencies and oxygen vacancies have both been observed.

Mohr salt analysis shows that DyFeO<sub>3</sub> ( $x = 0$ ) is a stoichiometric compound and the rest of the samples are nonstoichiometric compounds. The quantity of Fe<sup>4+</sup> increases with increase in  $x$ . Table II shows that the sample with  $x = 1$  has the nonstoichiometric formula SrFe<sub>0.54</sub><sup>3+</sup>Fe<sub>0.46</sub><sup>4+</sup>O<sub>2.73</sub>. MacChesney *et al.* (8, 9) produced a series of strontium ferrate compositions ranging from SrFeO<sub>2.7</sub> to SrFeO<sub>3.0</sub>, and the specimen SrFeO<sub>2.84</sub> was obtained by slow cooling from 1400°C to room temperature in 0.2 atm of oxygen. As we prepared the sample by air quenching from 1200°C to room temperature, SrFeO<sub>2.73</sub> was obtained. In order to make a stoichiometric solid solution SrFeO<sub>3</sub>, the sample must be annealed under high oxygen pressure. The concentration of oxygen vacancies is dependent upon the oxygen pressure and temperature at which samples are equilibrated and upon the cooling condition (3–10).

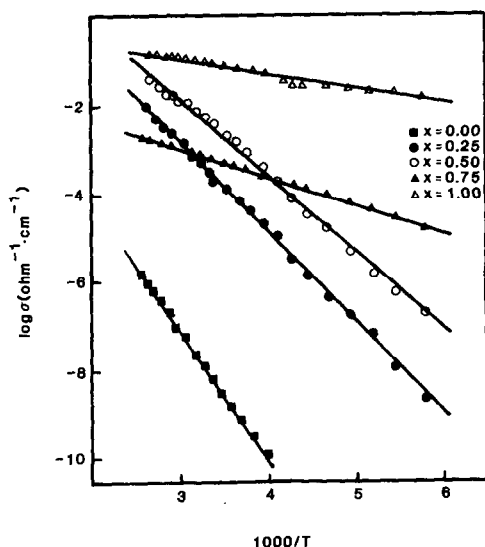


FIG. 2. Plot of log conductivity vs  $1000/T$  in the system  $\text{Sr}_x\text{Dy}_{1-x}\text{FeO}_{3-y}$ .

Electrical conductivity as a function of temperature is shown in Fig. 2. The conductivity of the ferrites containing  $\text{Sr}^{2+}$  is considerably higher than that of  $\text{DyFeO}_3$  due to the mixed valency of Fe. With increase in  $x$  value, the electrical conductivity at a constant temperature tends to increase, and the activation energy is decreased (5, 9, 11) (Table III). Such a change in electrical conductivity is due to

TABLE III  
ACTIVATION ENERGIES OF THE SYSTEM  
 $\text{Sr}_x\text{Dy}_{1-x}\text{FeO}_{3-y}$  AS A FUNCTION OF  $x$  VALUES

Composition ( $x$ )	Activation energy (eV)
0.00	0.54
0.25	0.39
0.50	0.35
0.75	0.16
1.00	0.07

electron hopping between  $\text{Fe}^{3+}$  and  $\text{Fe}^{4+}$  ions.

The Mössbauer spectrum of  $\text{DyFeO}_3$  is a six-line pattern characteristic of antiferromagnetic compounds below its Néel temperature. The reported values of isomer shift (I.S.), quadrupole splitting ( $E_Q$ ), and internal magnetic field ( $H_{\text{int}}$ ) at 296 K are 0.54 (mm/sec), 0.25 (mm/sec), and 498 ( $\text{KO}_e$ ), respectively (1, 2) (Table IV). The samples with  $x = 0.25$  and 0.50 yielded 12-line spectra. The intensities of the six new peaks are larger for  $x = 0.50$  than for  $x = 0.25$ . However,  $\text{Fe}^{4+}$  in  $x = 0.25$  and 0.50 could not be detected by Mössbauer effect, supposedly because the Mössbauer spectroscopy cannot always detect separately the mixed valencies on account of the rapid electronic exchange between them. As dis-

TABLE IV  
MÖSSBAUER PARAMETERS FOR COMPOSITIONS IN THE SYSTEM  $\text{Sr}_x\text{Dy}_{1-x}\text{FeO}_{3-y}$   
( $x = 0.25, 0.50, \text{ AND } 0.75$ )

Composition ( $x$ )	Temperature (K)	CN	I.S. (mm/sec)	$E_Q$ (mm/sec)	$H_{\text{int}}$ ( $\text{KO}_e$ )
0.25	95	6	0.36	-0.07	520
		4	0.38	0.03	416
0.50	95	6	0.45	-0.01	547
		4	0.36	0.03	453
0.75	295	6	0.32	0.39	—
		4	0.35	1.19	—
		$\text{Fe}^{4+}$	0.09	—	—
	95	6	0.33	0.59	—
		4	0.29	1.21	—
$\text{Fe}^{4+}$		0.12	—	—	

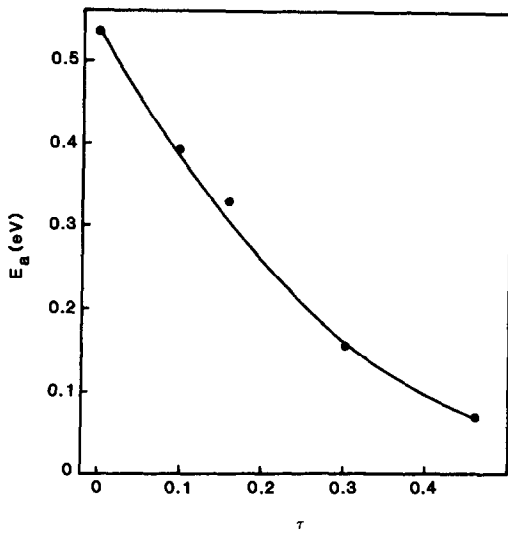


FIG. 3. Plot of  $E_a$  vs  $\tau$  values for the system Sr<sub>x</sub>Dy<sub>1-x</sub>FeO<sub>3-y</sub>. ( $\tau$ : amount of Fe<sup>4+</sup> ion.)

cussed by Yamamura (6, 12), the new six-line pattern was attributed to Fe<sup>3+</sup> in a tetrahedral site.

In the case of  $x = 0.75$ , a broad peak appears ranging from 0 to 0.9 mm/sec. As there are at least three distinct species of iron, the assignment of the spectra is complex (10, 11, 13) with two doublets from Fe<sup>3+</sup> at octahedral and tetrahedral sites and

possibly a peak from Fe<sup>4+</sup> (11). The idea of average valence state suggested by Takano *et al.* (4) may also be applicable to this system. Figure 6 shows that the Néel temperature of the sample  $x = 0.75$  is lower than 95 K, because the six-line pattern has disappeared. In the case of DyFeO<sub>3</sub>, the stability of the magnetic structure is ensured by  $e_g-P_0-e_g$  and  $t_{2g}-P_\pi-t_{2g}$  antiferromagnetic superexchange interaction. The partial substitution of Fe<sup>3+</sup> by Fe<sup>4+</sup> introduces ferromagnetic Fe<sup>3+</sup>-O-Fe<sup>4+</sup> and Fe<sup>4+</sup>-O-Fe<sup>4+</sup> interactions. So, with increasing  $x$ ,  $T_N$  decreases due to the competition of the antiferromagnetic couplings with ferromagnetic superexchange interaction.

## Results

The X-ray patterns after heat treatment confirmed that each sample was single phase. The cell parameters show that a change from orthorhombic to cubic symmetry occurs for a value of  $x$  intermediates between 0.25 and 0.50. The volume of the cell increases with  $x$  up to  $x = 0.75$ , then contract slightly for  $x = 1.00$ . Table II shows that both the amount of Fe<sup>4+</sup> and of oxygen deficiency increases with Sr content. Figure 2 shows the electrical conduc-

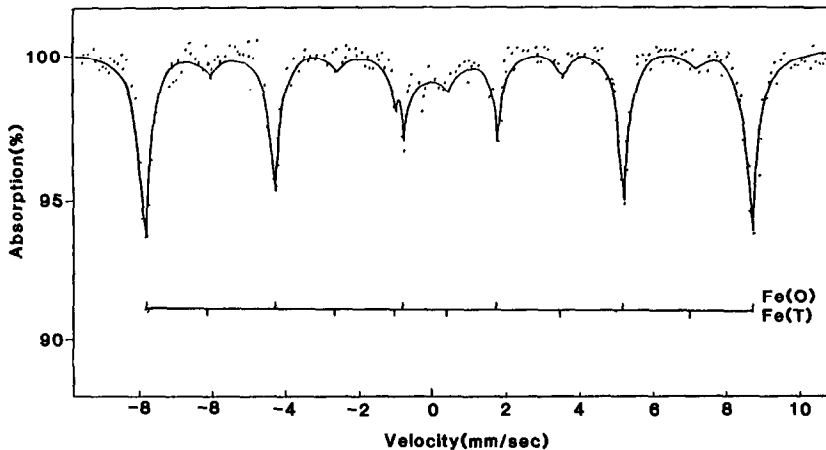


FIG. 4. Mössbauer spectrum of Sr<sub>0.25</sub>Dy<sub>0.75</sub>FeO<sub>2.925</sub> at 95 K.

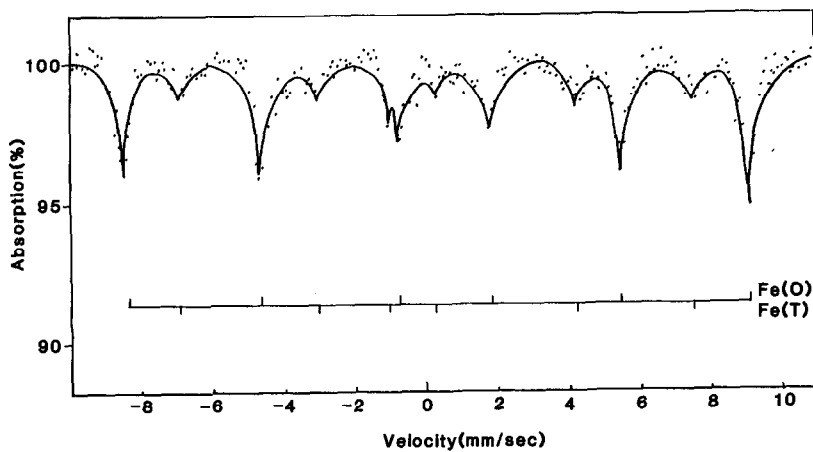


FIG. 5. Mössbauer spectrum of  $\text{Sr}_{0.50}\text{Dy}_{0.50}\text{FeO}_{2.830}$  at 95 K.

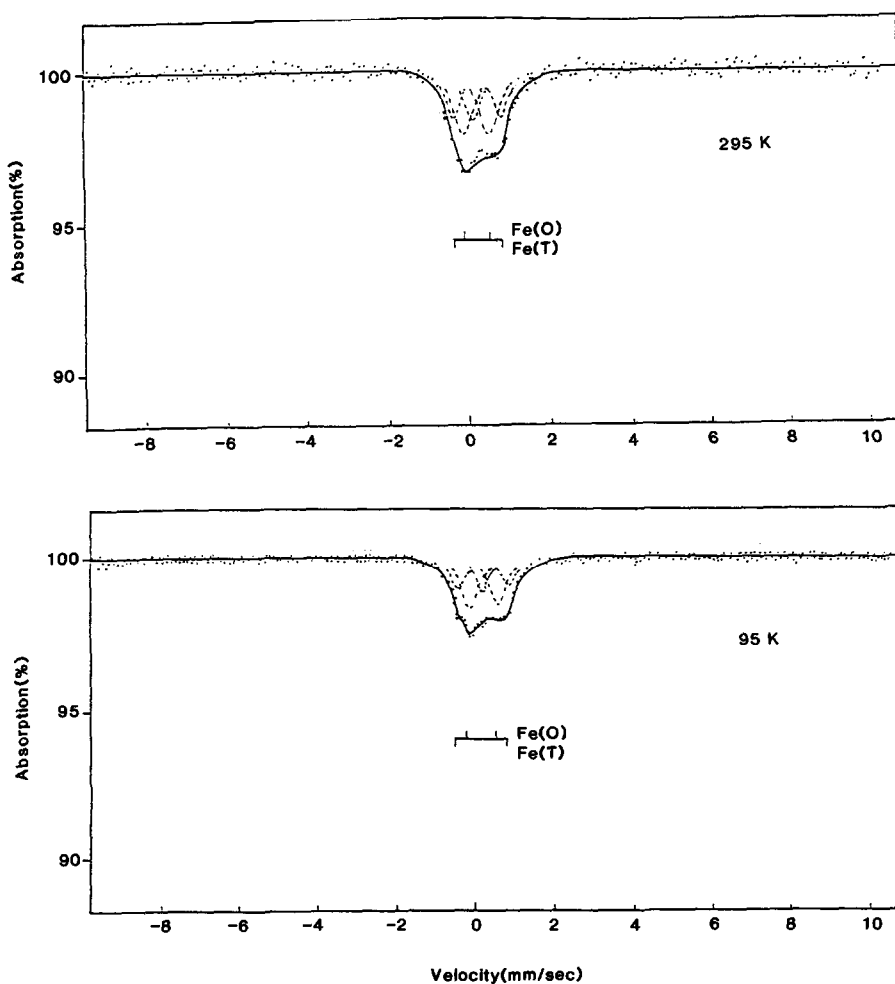


FIG. 6. Mössbauer spectra of  $\text{Sr}_{0.75}\text{Dy}_{0.25}\text{FeO}_{2.775}$  at 295 and 95 K.

tivity for temperatures within the range 173 ~ 473 K. Activation energies ( $E_a$ ), calculated from the slope of each line using the relations for the various temperature regions, decrease with an increase in  $\tau$  value (Fig. 3). Mössbauer spectra of the system ( $x = 0.25, 0.50,$  and  $0.75$ ) are shown in Figs. 4–6.

### Acknowledgments

We express our appreciation to Korea Science and Engineering Foundation for financial assistance and to Professor Hang Nam Ok for the Mössbauer measurements.

### References

1. M. EIBSCHUTZ, S. SHTRIKMAN, AND D. TREVES, *Phys. Rev.* **2**, 156 (1967).
2. D. TREVES, *J. Appl. Phys.* **36**, 1033 (1965).
3. H. WATANABE, *J. Phys. Soc. Japan* **12**, 515 (1957).
4. M. TAKANO, J. KAWACHI, N. NAKANISHI, AND Y. TAKEDA, *J. Solid State Chem.* **39**, 75 (1981).
5. U. SHIMONY AND JENS M. KNUDSEN, *Phys. Rev.* **144**, 361 (1966).
6. H. YAMAMURA AND R. KIRIYAMA, *Bull. Chem. Soc. Japan* **45**, 2702 (1972).
7. J. LAPLUME, *L'onde Electrique*, **35**, 113 (1955).
8. P. K. GALIAGHER, J. B. MACCHESNEY, AND D. N. E. BUCHANAN, *J. Chem. Phys.* **41**, 2429 (1964).
9. J. B. MACCHESNEY, R. C. SHERWOOD, AND J. F. POTTER, *J. Chem. Phys.* **43**, 1907 (1965).
10. P. K. GALIAGHER, J. B. MACCHESNEY, AND D. N. E. BUCHANAN, *J. Chem. Phys.* **45**, 2466 (1966).
11. F. MENIL, N. KINOMURA, L. FOURNES, J. PORTIER, AND P. HAGENMULLER, *Phys. Status Solidi* **64**, 261 (1981).
12. H. YAMAMURA, H. HANEDA, AND S. SHIRASAKI, *J. Solid State Chem.* **36**, 1 (1981).
13. J. C. GRENIER, F. MENIL, M. POUCHARD, AND P. HAGENMULLER, *Mater. Res. Bull.* **13**, 329 (1978).